

**WAVE FIELD EXTRAPOLATION TECHNIQUES  
FOR INHOMOGENEOUS MEDIA WHICH INCLUDE  
CRITICAL ANGLE EVENTS.  
PART III: APPLICATIONS IN MODELING,  
MIGRATION AND INVERSION\***

C.P.A. WAPENAAR and A.J. BERKHOUT\*\*

**ABSTRACT**

WAPENAAR, C.P.A. and BERKHOUT, A.J. 1986, Wave Field Extrapolation Techniques for Inhomogeneous Media which Include Critical Angle Events. Part III: Applications in Modeling, Migration and Inversion, Geophysical Prospecting 34, 180–207.

Wave field extrapolation including critical angle events in modeling, migration and inversion can be handled with algorithms based on both the one-way wave equations and the two-way wave equation. It is shown that for 1-D inhomogeneous media, critical angle events as well as multiple reflections may elegantly be included in pre-stack modeling, pre-stack migration and velocity inversion. For 2-D and 3-D inhomogeneous media a powerful pre-stack migration scheme can be developed which includes critical angle events as well as multiple reflections. Finally, suggestions for practical applications are given.

**1. INTRODUCTION**

It has been shown by Berkhou (1982) that a seismic experiment can be elegantly described by a sequence of independent one-way processes, which is schematically represented by

$$S \rightarrow W^+ \rightarrow R \rightarrow W^- \rightarrow D \rightarrow P. \quad (1.1)$$

A wave field, generated by sources  $S$  at the surface, propagates downward into the earth, which is described by one-way wave field extrapolation operator  $W^+$ . In the subsurface this wave field is reflected, described by  $R$ , and propagates upward to the surface again, described by one-way operator  $W^-$ . At the surface the wave field is registered by detectors  $D$ , resulting in a seismic section  $P$ . This simplified model is

\* Received December 1984, revision accepted July 1985.

\*\* T.H. Delft, Laboratory of Seismics and Acoustics, PB 5046, 2600 GA Delft, The Netherlands.

valid for sub-critical angle events only, as interaction between downgoing and upgoing waves is neglected. Based on this model, Berkhout discussed modeling as well as migration schemes for sub-critical data in 1-D, 2-D and 3-D inhomogeneous media. We generalized relation (1.1) (Wapenaar and Berkhout 1985) such that critical angle events may be included in 1-D inhomogeneous media, according to

$$S \rightarrow \mathcal{W}^+ \rightarrow \mathcal{R} \rightarrow \mathcal{W}^- \rightarrow D \rightarrow P. \quad (1.2)$$

Here  $\mathcal{W}^+$  and  $\mathcal{W}^-$  represent WKBJ one-way wave field extrapolation operators which include sub-critical as well as critical angle events, while  $\mathcal{R}$  describes the reflectivity at the turning point. This improved one-way approach breaks down for 2-D and 3-D inhomogeneous media. Therefore, in part II (Wapenaar and Berkhout 1986a) we discussed the two-way approach to wave field extrapolation, which is schematically represented by

$$\begin{bmatrix} P \\ \frac{1}{\rho} \frac{\partial P}{\partial z} \end{bmatrix}_{z_1} \rightarrow \mathbf{W} \rightarrow \begin{bmatrix} P \\ \frac{1}{\rho} \frac{\partial P}{\partial z} \end{bmatrix}_{z_2}. \quad (1.3)$$

Here  $[P, \rho^{-1} \partial_z P]^T$  describes the *total* wave field, while  $\mathbf{W}$  describes the two-way wave propagation effects (downgoing source waves and upgoing reflected waves) between two depth levels. (1.3) holds for subcritical as well as critical angle events in 1-D, 2-D and 3-D inhomogeneous media. In part III we present various pre-stack modeling, migration and inversion algorithms based on (1.2) and (1.3). For notation convenience we often denote a wave field  $P(x, y, z_i, \omega)$  in the space-frequency domain as  $P(z_i)$  or  $P$ , while a wave field  $\tilde{P}(k_x, k_y, z_i, \omega)$  in the wave number-frequency domain is often denoted as  $\tilde{P}(z_i)$  or  $\tilde{P}$ . Similar conventions are used for operators.

## 2. MODELING SCHEME BASED ON THE ONE-WAY WAVE EQUATIONS

We discuss a recursive modeling scheme based on the WKBJ *one-way* wave equations for 1-D inhomogeneous media, where primary and multiple energy as well as critical angle events are included. A similar scheme for sub-critical angle events in 2-D and 3-D inhomogeneous media is discussed by Berkhout (1982).

We consider a horizontally layered medium consisting of  $M$  (vertically inhomogeneous) *macro* layers (fig. 1). We assume homogeneous half spaces for  $z < z_0$  and  $z \geq z_M$ . Throughout this paper, the  $z$ -axis is pointing downward. In layer  $m + 1$ , with  $z_m \leq z < z_{m+1}$ , the propagation velocity and the density is given by  $c_{m+1}(z)$  and  $\rho_{m+1}(z)$ , respectively. These are continuous monotonous functions of depth, with vanishing gradients in the vicinity of the interfaces. Notice that the concept "vicinity of an interface" is related to the seismic frequency content. This means that the assumed gradient-free area around the interfaces is proportional to the largest local wave length under consideration.

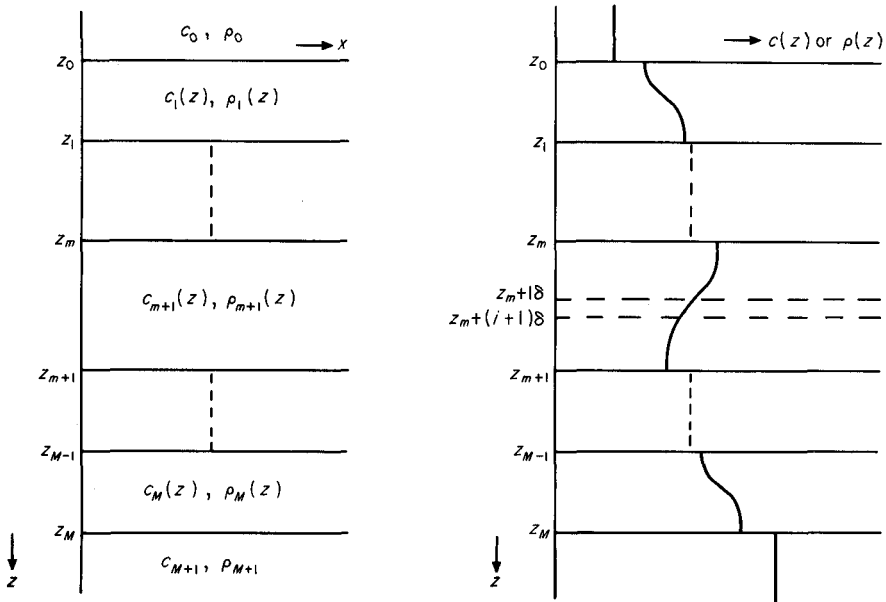


Fig. 1. Acoustic model of the subsurface for the one-way wave equation modeling scheme which includes critical angle events.

In the wave number-frequency domain  $(k_x, k_y, \omega)$ , modeling consists of the following steps:

1. given the impulse response  $\tilde{X}(z_{m+1})$  for the lower half space  $z \geq z_{m+1}$ , then the *primary* waves in layer  $m + 1$  can be modeled according to

$$\tilde{X}^{(0)}(z_m) = \tilde{W}^-(z_m, z_{m+1})[\tilde{X}(z_{m+1} - \epsilon) + \tilde{R}(z_{m+1})]\tilde{W}^+(z_{m+1}, z_m), \tag{2.1}$$

with  $\epsilon \rightarrow 0$ . The extrapolation operators  $\tilde{W}^+$  and  $\tilde{W}^-$  as well as the reflection operator  $\tilde{R}$  are discussed below;

2. given  $\tilde{X}^{(0)}(z_m)$ , then the *multiples* related to interface  $z = z_m$  can be optionally included according to

$$\tilde{X}(z_m) = [1 - \tilde{X}^{(0)}(z_m)\tilde{R}^-(z_m)]^{-1}\tilde{X}^{(0)}(z_m). \tag{2.2}$$

Multiple generation, as described by (2.2), is schematically shown in fig. 2. Notice that the reflection operator  $\tilde{R}^-(z_m) = -\tilde{R}(z_m)$  describes reflection at the lower side of interface  $z_m$ .

Steps 1 and 2, which describe the total modeling procedure for layer  $m + 1$ , should be applied recursively;

3. the procedure (for each  $k_x, k_y$  and  $\omega$ -value) starts at the shallowest level  $z$ , where total reflection occurs, or at the maximum depth  $z = z_M$  if total reflection does not occur.

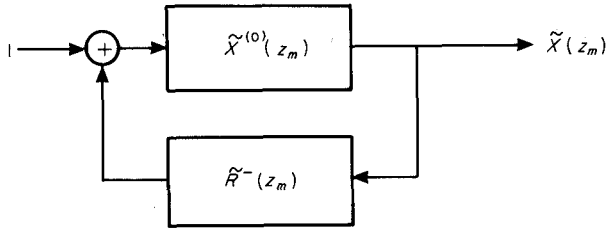


Fig. 2. Feed-back system for multiple generation at interface  $m$ .

4. when the surface  $z = z_0$  has been reached, then the source and detector properties can be included, according to

$$\tilde{P}_{CSG}^-(z_0) = \tilde{D}(z_0)\tilde{X}(z_0)\tilde{S}^+(z_0), \tag{2.3}$$

where  $\tilde{S}^+(z_0)$  represents the downgoing source pressure wave,  $\tilde{D}(z_0)$  represents the detector transfer function and  $\tilde{P}_{CSG}^-(z_0)$  represents the detected upgoing pressure wave in a Common Shot Gather (CSG);

5. when this modeling procedure has been applied for all wave numbers and frequencies, then the space-time data (one shot record) are obtained after inverse Fourier transforms.

*Discussion*

The extrapolation operators  $\tilde{W}$  in (2.1) are composed of  $N$  sub-operators, according to

$$\tilde{W}^+(z_{m+1}, z_m) = \prod_{i=0}^{N-1} \tilde{W}^+[z_m + (i + 1)\delta, z_m + i\delta], \tag{2.4a}$$

$$\tilde{W}^-(z_m, z_{m+1}) = \prod_{i=0}^{N-1} \tilde{W}^-[z_m + i\delta, z_m + (i + 1)\delta], \tag{2.4b}$$

with  $\delta = (z_{m+1} - z_m)/N$ . If in each *micro* layer  $[z_m + i\delta \leq z < z_m + (i + 1)\delta]$  the operator  $\tilde{H}_2(z) = \omega^2/c^2(z) - k_x^2 - k_y^2$  may be linearized in  $z$ , the sub-operators represent LG-operators for sub-critical angle events given by (5.11a, b) in part I if  $\tilde{H}_2(z)$  is sufficiently large positive; they represent WKBJ operators  $\tilde{W}^+$  and  $\tilde{W}^-$  for critical angle events given by (7.6c, d) in part I if  $\tilde{H}_2(z)$  is small positive. Notice that we assume propagating waves for  $z_m \leq z < z_{m+1}$ .

Recall that the LG-operators are based on wave functions, developed by Liouville and Green in 1837, which hold away from a turning point. The WKBJ-operators are based on wave functions, developed by Wentzel, Kramers, Brillouin and Jeffreys in 1924–1926, which hold close to and at a turning point (see part I).

An expression for  $\tilde{X}(z_{m+1} - \epsilon)$ ,  $\epsilon \rightarrow 0$ , in (2.1), is given by

$$\lim_{\epsilon \rightarrow 0} \tilde{X}(z_{m+1} - \epsilon) = \tilde{T}^-(z_{m+1})\tilde{X}(z_{m+1})\tilde{T}^+(z_{m+1}), \tag{2.5a}$$

$$\tilde{T}^\pm(z_{m+1}) = 1 \pm \tilde{R}(z_{m+1}), \tag{2.5b}$$

where  $\tilde{T}^+$ ,  $\tilde{T}^-$  and  $\tilde{R}$  describe the transmission and reflection properties of the interface, with  $\tilde{R}$  given by (AI.3b) in part I.

The shallowest level  $z_t$  where total reflection occurs, as introduced in step 3, can represent an interface or a turning point. In the latter case,  $z_t$  generally lays inside a macro layer ( $z_m < z_t < z_{m+1}$ ), with  $\tilde{H}_2(z_t) = 0$ . Now the recursion procedure starts with

$$\tilde{X}^{(0)}(z_m) = \tilde{W}^-(z_m, z_t)\tilde{\mathcal{R}}(z_t)\tilde{W}^+(z_t, z_m),$$

where  $\tilde{\mathcal{R}}(z_t)$  describes the reflectivity at the turning point, given by (7.9b) in part I, while the operators  $\tilde{W}^+$  and  $\tilde{W}^-$  are again composed of LG and WKBJ operators, similar as in (2.4).

Notice that in the critical angle modeling scheme as introduced in this section, evanescent waves are neglected. This is justified if—as assumed—

- (i) macro layers are considered;
- (ii) the velocity gradients vanish in the vicinity of the interfaces, so no turning points are present in this area; and
- (iii) the velocity functions are continuous monotonous, so not more than one turning point is present in each macro-layer.

A similar *modeling* scheme for piecewise smooth models is presented by Kennett and Illingworth (1981). The main difference of both approaches lies in the formulation. Our approach is basically founded on model (1.2):

$$S \rightarrow \mathcal{W}^+ \rightarrow \mathcal{R} \rightarrow \mathcal{W}^- \rightarrow D \rightarrow P$$

and therefore it provides an excellent starting point for the critical angle *migration* scheme, as discussed in section 5.

For more complicated velocity models, a two-way wave equation modeling scheme is preferred. This is discussed in the next section, where also a numerical example is given for the more general case.

### 3. MODELING SCHEME BASED ON THE TWO-WAY WAVE EQUATION

In this section we discuss a recursive modeling scheme, based on the *two-way* wave equation, which includes primary and multiple energy as well as critical angle events.

We consider a horizontally layered medium consisting of  $I$  (inhomogeneous) *micro* layers, as is shown in fig. 3. We assume homogeneous half-spaces for  $z < z_0$  and  $z \geq z_I$ . In layer  $i + 1$ , with  $z_i \leq z < z_{i+1}$ , the propagation velocity and density be given by  $c_{i+1}(z)$  and  $\rho_{i+1}(z)$ , respectively. As we consider micro layers we assume that these functions may be linearized in  $z$ .

In the wave number-frequency domain, modeling consists of the following steps:

1. given the total field  $\tilde{\mathbf{Q}}(z_{i+1})$ , all *propagation effects* for layer  $i + 1$  can be modeled according to

$$\tilde{\mathbf{Q}}(z_i) = \tilde{\mathbf{W}}(z_i, z_{i+1})\tilde{\mathbf{Q}}(z_{i+1}), \quad (3.1)$$

with  $\tilde{\mathbf{Q}} = [\tilde{\mathbf{P}}, \rho^{-1} \partial_z \tilde{\mathbf{P}}]^T = [\tilde{\mathbf{P}}, -j\omega \tilde{\mathbf{V}}_z]^T$ , and  $\tilde{\mathbf{W}}$  being given by (3.9) in part II.

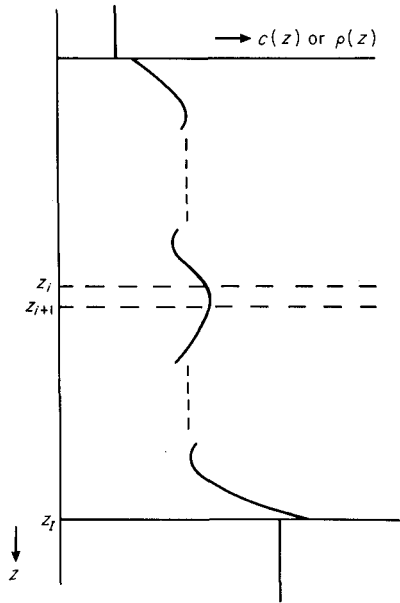


Fig. 3. Acoustic model of the subsurface for the two-way wave equation modeling scheme which includes critical angle events.

Step 1, which describes the total modeling procedure for layer  $i + 1$ , should be applied recursively; this is allowed because  $\tilde{\mathbf{Q}}$  is continuous for all depths;

2. the procedure starts at  $z = z_l$  by specifying  $\tilde{\mathbf{Q}}(z_l)$ , according to

$$\tilde{\mathbf{Q}}(z_l) = \tilde{\mathbf{L}}(z_l)\tilde{\mathbf{P}}(z_l), \tag{3.2}$$

with  $\tilde{\mathbf{P}} = [\tilde{\mathbf{P}}^+, \tilde{\mathbf{P}}^-]^T$ , and  $\tilde{\mathbf{L}}$  being given by (3.3b) in part II. Since the lower half space  $z \geq z_l$  is homogeneous, the upgoing wave  $\tilde{\mathbf{P}}^-(z_l)$  should be taken zero;

3. when the surface  $z = z_0$  has been reached, the impulse response can be calculated from  $\tilde{\mathbf{Q}}(z_0) = [\tilde{\mathbf{P}}(z_0), -j\omega\tilde{\mathbf{V}}_z(z_0)]^T$ . We consider two cases;

(i) we define the impulse response  $\tilde{\mathbf{X}}(z_0)$  which describes the detected upgoing pressure wave due to an impulsive downgoing pressure source wave, according to

$$\tilde{\mathbf{P}}(z_0) = [\tilde{\mathbf{P}}^+(z_0), \tilde{\mathbf{P}}^-(z_0)]^T = \tilde{\mathbf{L}}^{-1}(z_0)\tilde{\mathbf{Q}}(z_0), \tag{3.3a}$$

$$\tilde{\mathbf{X}}^{(0)}(z_0) = \tilde{\mathbf{P}}^-(z_0)/\tilde{\mathbf{P}}^+(z_0), \tag{3.3b}$$

$$\tilde{\mathbf{X}}(z_0) = [1 - \tilde{\mathbf{X}}^{(0)}(z_0)\tilde{\mathbf{R}}^-(z_0)]^{-1}\tilde{\mathbf{X}}^{(0)}(z_0), \tag{3.3c}$$

where we assumed micro layer 1 to be homogeneous;

(ii) if  $z_0$  is a (pressure) free surface, we prefer an admittance impulse response

$\tilde{Y}(z_0)$  which describes the detected total particle velocity due to an impulsive pressure source. We may simply write

$$\tilde{Y}(z_0) = \tilde{V}_z(z_0)/\tilde{P}(z_0), \tag{3.4}$$

since at a free surface the total pressure is given by the source pressure only;

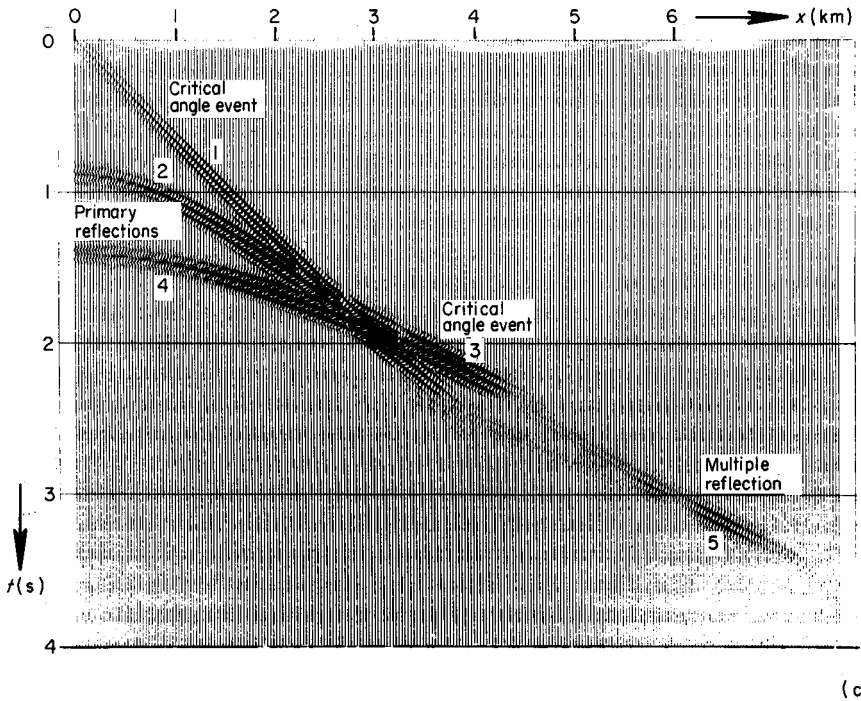
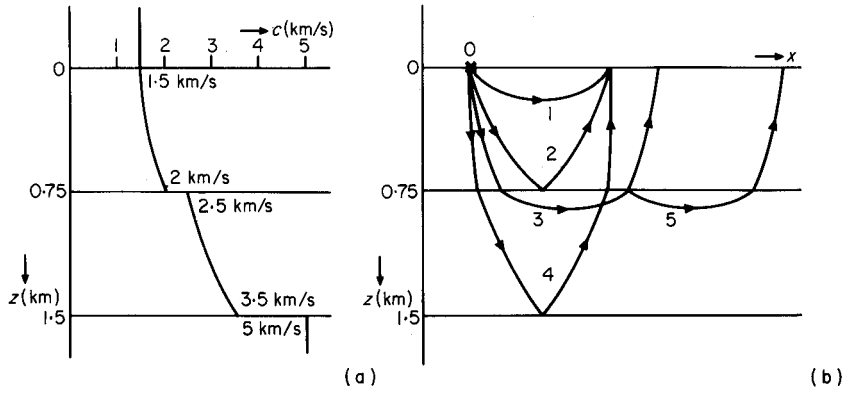


Fig. 4. Critical angle data, modeled with the two-way wave equation. (a) Subsurface velocity model (density is constant). (b) Ray-representation. (c) CSG in  $x, t$ -domain.

4. next the source and detector properties can be included. Again we consider two cases:

(i) we write for the detected upgoing pressure wave in a Common Shot Gather

$$\tilde{P}_{\text{CSG}}^-(z_0) = \tilde{D}(z_0)\tilde{X}(z_0)\tilde{S}^+(z_0), \quad (3.5)$$

with  $\tilde{S}^+(z_0)$  and  $\tilde{D}(z_0)$  defined in section 2;

(ii) for the detected particle velocity in a Common Shot Gather at a pressure free surface we may write

$$\tilde{V}_{z, \text{CSG}}(z_0) = \tilde{D}(z_0)\tilde{Y}(z_0)\tilde{S}(z_0), \quad (3.6)$$

where  $\tilde{S}(z_0)$  represents the pressure source and  $\tilde{D}(z_0)$  represents the particle velocity detector transfer function;

5. when this modeling procedure has been applied for all wave numbers and frequencies, the space-time data are obtained after inverse Fourier transforms.

Notice that in step 2 the downgoing wave  $\tilde{P}^+(z_I)$  can be chosen arbitrarily, e.g.,  $\tilde{P}(z_I) = [1, 0]^T$ , because in step 3 the ratios  $\tilde{P}^-/\tilde{P}^+$  or  $\tilde{V}_z/\tilde{P}$  are considered.

A two-dimensional Common Shot Gather was modeled for the 1-D subsurface configuration shown in fig. 4a. Figure 4b shows the ray representation, while fig. 4c represents the CSG in the space-time domain  $(x, t)$ . Notice that sub-critical angle events (2, 4) as well as critical angle events (1, 3) and multiple reflection (5) are clearly visible in fig. 4c. Of course, more multiples are present; they are not visible due to their very low amplitudes.

The advantage of the scheme introduced in this section over that introduced in the previous section is that critical angle events, multiple reflections, transmission effects as well as evanescent energy are all included in the simple recursion algorithm (3.1) and that arbitrary 1-D piecewise continuously layered media can be handled (compare figs 1 and 3). Based on the same concept, a two-way wave equation modeling scheme for *full elastic media* is presented by Wapenaar and Berkhout (1986b).

#### 4. PRE-STACK MIGRATION, GENERAL CONSIDERATIONS

In principle all migration schemes are based on the following two steps:

1. downward extrapolation;
2. imaging.

We briefly discuss these steps for various migration schemes.

The best known scheme is the *post-stack* migration scheme based on the exploding reflector model (Loewenthal, Lu, Roberson and Sherwood 1974). The stacked (pseudo zero-offset) data are considered as an upgoing wave field  $P^-(z_0)$  which is radiated at  $t = 0$  by sources inside the medium. The source strength distribution is assumed to be proportional to the zero-offset reflectivity distribution  $R(x, y, z)$ .

For post-stack migration, the two basic steps can be specified as follows:

1. downward extrapolation involves inverse extrapolation of the upgoing wave field using half the propagation velocity, yielding  $P^-(z_i)$ ;
2. imaging involves integration over all frequencies in order to resolve the wave field at  $t = 0$ , according to

$$\langle R(x, y, z_i) \rangle = \frac{1}{2\pi} \int_{\omega} P^-(x, y, z_i, \omega) d\omega. \quad (4.1)$$

The procedure is repeated (recursively or non-recursively) for all depths  $z_i$ .

Of all *pre-stack* migration schemes, the Single Shot Record Inversion (SSRI) scheme proposed by Berkhout (1982) seems to be the most promising one, for both 2-D and 3-D applications, since individual seismic experiments (which obey the wave equation) are migrated, while true Common Depth Point (CDP) stacking is accomplished.

We specify the two recursion steps for pre-stack migration by SSRI.

1. Downward extrapolation should be applied to a single CSG. We consider two cases:

- (i) apply forward extrapolation to the downgoing source wave, based on the one-way wave equation for downgoing waves, yielding  $S^+(z_i)$ . Apply inverse extrapolation to the upgoing detected wave, based on the one-way wave equation for upgoing waves, yielding  $P^-(z_i)$ ;
- (ii) alternatively, apply downward extrapolation to the total wave field, based on the two-way wave equation, followed by decomposition, yielding  $S^+(z_i)$  and  $P^-(z_i)$ .

The first approach is very robust, and may handle sub-critical as well as critical angle events (the latter only in 1-D inhomogeneous media). The second approach may handle multiple reflections, transmission effects, wave conversion (optionally), and sub-critical as well as critical angle events, but is less robust.

2. Imaging can be applied either in the space-frequency domain or in the wave number-frequency domain:

- (i) in the space-frequency domain, ZO-imaging involves integration of the Zero Offset (ZO) impulse response  $X$  over all frequencies in order to resolve the ZO-reflectivity at the current level (downgoing and upgoing waves are time-coincident), according to

$$\langle R(x, y, z_i) \rangle = \frac{1}{2\pi} \int_{\omega} X(x, y, z_i, \omega) d\omega, \quad (4.2a)$$

where

$$X(x, y, z_i, \omega) \triangleq P^-(x, y, z_i, \omega)/S^+(x, y, z_i, \omega) \quad (4.2b)$$

in some stable sense. The integration is carried out for constant  $x$  and  $y$ ;

- (ii) alternatively, imaging in the wave number-frequency domain involves integra-

tion of the Plane Wave (PW) impulse response  $\tilde{X}$  over all frequencies, in order to resolve the PW-reflectivity at the current level, according to

$$\langle \tilde{R}(p_x, p_y, z_i) \rangle = \frac{1}{2\pi} \int_{\omega} \tilde{X}(k_x, k_y, z_i, \omega) d\omega, \quad (4.3a)$$

where

$$\tilde{X}(k_x, k_y, z_i, \omega) \cong \tilde{P}^-(k_x, k_y, z_i, \omega) / \tilde{S}^+(k_x, k_y, z_i, \omega) \quad (4.3b)$$

in some stable sense. The symbol  $\int'$  denotes that the integration is carried out for constant  $p_x = k_x/\omega$  and  $p_y = k_y/\omega$  (constant propagation angle).

In media with strongly *laterally* varying reflection properties, ZO-imaging should be applied according to (4.2). On the other hand, in media with purely *vertically* varying medium properties, PW-imaging should preferably be applied according to (4.3), particularly when angle dependent turning point problems are considered. When *both* lateral and vertical variations of the medium properties are important, then the choice of the imaging principle depends on the relevant migration objectives.

The procedure is repeated (recursively or non-recursively) for all depths  $z_i$ . In case of laterally varying reflection properties, steps 1 and 2(i) should be repeated for all CSG's. The individual migration results can be summed afterward (true CDP-stacking), optionally after a residual NMO-correction if the input velocity model is in error.

## 5. PRE-STACK MIGRATION SCHEME BASED ON THE ONE-WAY WAVE EQUATIONS

De Graaff (1984) discussed a single record pre-stack migration scheme for sub-critical angle events in 2-D inhomogeneous media, based on the *one-way* wave equations and ZO-imaging. In this section we discuss a single record pre-stack migration scheme which includes critical angle events, based on the WKB *one-way* wave equations for 1-D inhomogeneous media and PW-imaging. We follow the approach discussed in section 4. The scheme is based on inversion of the modeling scheme discussed in section 2. When interface related multiples as well as transmission effects are neglected, then this modeling scheme can be summarized by

$$\tilde{P}_{\text{CSG}}^-(z_0) = \tilde{D}(z_0) \tilde{X}(z_0) \tilde{S}^+(z_0), \quad (5.1a)$$

where

$$\tilde{X}(z_0) = \sum_m \tilde{W}^-(z_0, z_m) \tilde{R}(z_m) \tilde{W}^+(z_m, z_0). \quad (5.1b)$$

The non-recursive operators  $\tilde{W}^+(z_m, z_0)$  and  $\tilde{W}^-(z_0, z_m)$  are composed of many sub-operators  $\tilde{W}^+[z_m + (i+1)\delta, z_m + i\delta]$  and  $\tilde{W}^-[z_m + i\delta, z_m + (i+1)\delta]$  for micro layers (see fig. 1), which may represent either LG or WKB operators  $\tilde{W}^+$  and  $\tilde{W}^-$ . The reflection operator  $\tilde{R}(z_m)$  can either describe reflection at an interface  $z_m$

between two macro layers, or total reflection  $\tilde{\mathcal{R}}(z_i)$  at a turning point  $z_i$  inside a macro layer. According to this model, the forward extrapolated source wave follows from

$$\tilde{S}^+(z_m + i\delta) = \tilde{W}^+(z_m + i\delta, z_0)\tilde{S}^+(z_0) \quad (5.2a)$$

while the inverse extrapolated detected wave follows from

$$\tilde{P}^-(z_m + i\delta) = [\tilde{D}(z_0)\tilde{W}^-(z_0, z_m + i\delta)]^{-1}\tilde{P}^-_{\text{CSG}}(z_0). \quad (5.2b)$$

From (5.1) and (5.2) it follows that the PW-impulse response may be written as

$$\begin{aligned} \tilde{X}(z_m + i\delta) &\triangleq \tilde{P}^-(z_m + i\delta)/\tilde{S}^+(z_m + i\delta) \\ &= [\tilde{W}^-(z_0, z_m + i\delta)]^{-1}\tilde{X}(z_0)[\tilde{W}^+(z_m + i\delta, z_0)]^{-1}, \end{aligned} \quad (5.3a)$$

where  $\tilde{X}(z_0)$  is implicitly defined by (5.1a). (5.3a) describes non-recursive downward extrapolation of the PW-impulse response. Similarly, for  $\tilde{X}[z_m + (i + 1)\delta]$  we may write

$$\tilde{X}[z_m + (i + 1)\delta] = \{\tilde{W}^-[z_0, z_m + (i + 1)\delta]\}^{-1}\tilde{X}(z_0)\{\tilde{W}^+[z_m + (i + 1)\delta, z_0]\}^{-1}, \quad (5.3b)$$

where

$$\tilde{W}^+[z_m + (i + 1)\delta, z_0] = \tilde{W}^+[z_m + (i + 1)\delta, z_m + i\delta]\tilde{W}^+(z_m + i\delta, z_0), \quad (5.3c)$$

$$\tilde{W}^-[z_0, z_m + (i + 1)\delta] = \tilde{W}^-[z_0, z_m + i\delta]\tilde{W}^-[z_m + i\delta, z_m + (i + 1)\delta]. \quad (5.3d)$$

Using these results, we propose the following recursive single record pre-stack one-way migration scheme, which includes critical angle events:

1. given the PW-impulse response  $\tilde{X}(z_m + i\delta)$ , then downward extrapolation can be applied, according to

$$\begin{aligned} \tilde{X}[z_m + (i + 1)\delta] \\ = \tilde{F}^-[z_m + (i + 1)\delta, z_m + i\delta]\tilde{X}(z_m + i\delta)\tilde{F}^+[z_m + i\delta, z_m + (i + 1)\delta], \end{aligned} \quad (5.4a)$$

with

$$\tilde{F}^+[z_m + i\delta, z_m + (i + 1)\delta] = [\tilde{W}^+]^{-1} = \{\tilde{W}^-[z_m + i\delta, z_m + (i + 1)\delta]\}^*, \quad (5.4b)$$

$$\tilde{F}^-[z_m + (i + 1)\delta, z_m + i\delta] = [\tilde{W}^-]^{-1} = \{\tilde{W}^+[z_m + (i + 1)\delta, z_m + i\delta]\}^*, \quad (5.4c)$$

where the symbol \* refers to complex conjugation;

2. PW-imaging can be applied, according to

$$\langle \tilde{R}[p_x, p_y, z_m + (i + 1)\delta] \rangle = \frac{\Delta\omega}{2\pi} \sum' \tilde{X}[k_x, k_y, z_m + (i + 1)\delta, \omega], \quad (5.5)$$

where the symbol  $\sum'$  denotes that the summation is carried out for constant  $p_x = k_x/\omega$  and  $p_y = k_y/\omega$ , and where  $\Delta\omega$  represents the circular frequency sampling interval.

Steps 1 and 2, which describe the total migration procedure for one micro-layer, should be applied recursively;

3. the procedure starts at  $z_0$ , where  $\tilde{X}(z_0)$  is estimated from the CSG, according to

$$\tilde{X}(z_0) = [\tilde{D}(z_0)]^{-1} \tilde{P}_{CSG}^-(z_0) [\tilde{S}^+(z_0)]^{-1}, \tag{5.6a}$$

where

$$[\tilde{S}^+(z_0)]^{-1} \approx [\tilde{S}^+(z_0)] * / [|\tilde{S}^+(z_0)|^2 + \sigma_1^2] \tag{5.6b}$$

and

$$[\tilde{D}(z_0)]^{-1} \approx [\tilde{D}(z_0)] * / [|\tilde{D}(z_0)|^2 + \sigma_2^2]. \tag{5.6c}$$

Here  $\sigma_1$  and  $\sigma_2$  represent stabilization constants. The scaling factors in (5.6b, c) may often be deleted because amplitude errors are less important than phase errors;

4. the procedure stops at the shallowest level where total reflection occurs, or at the maximum depth  $z = z_M$  if total reflection does not occur.

*Discussion*

In the procedure described above it is assumed that the CSG has been transformed to the wave number-frequency domain. Both the extrapolation (step 1) and imaging (step 2) take place in the wave number-frequency domain. Imaging for constant  $p = k_x/\omega$  is visualized in fig. 5a, assuming a 2-D situation. Alternatively, the original CSG can be slant-stacked ( $p, \tau$ -transformation), followed by a temporal Fourier transform, yielding the CSG in the ray parameter-frequency domain ( $p, \omega$ ). Now, in the operators for downward extrapolation (step 1),  $k_x$  should be replaced by  $p\omega$ . Imaging for constant  $p$  (step 2) is visualized in fig. 5b. The final migration output of both approaches should be identical and represent the reflectivity distribution in

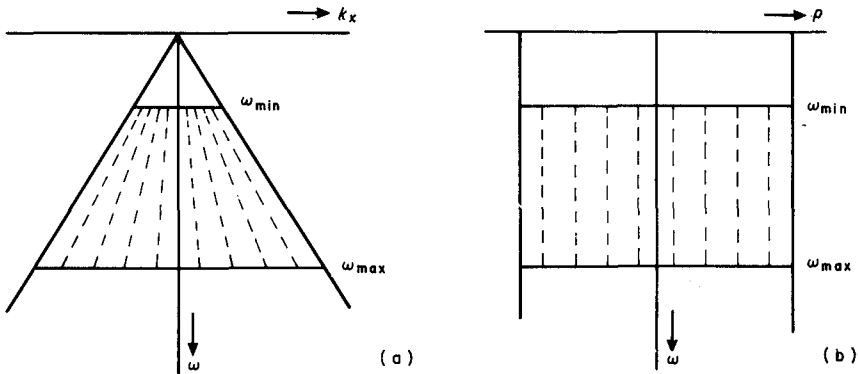


Fig. 5. Two approaches to the plane wave imaging principle. (a) Summation along lines of constant  $k_x/\omega$  in the  $k_x, \omega$ -domain. (b) Summation along lines of constant  $p$  in the  $p, \omega$ -domain.

the ray parameter-depth domain ( $p, z$ ). Theoretically, the one-way wave equation migration scheme assumes the model of fig. 1. In practice, however, sufficient accuracy is obtained when the generalized model of fig. 3 is assumed. Figure 6a rep-

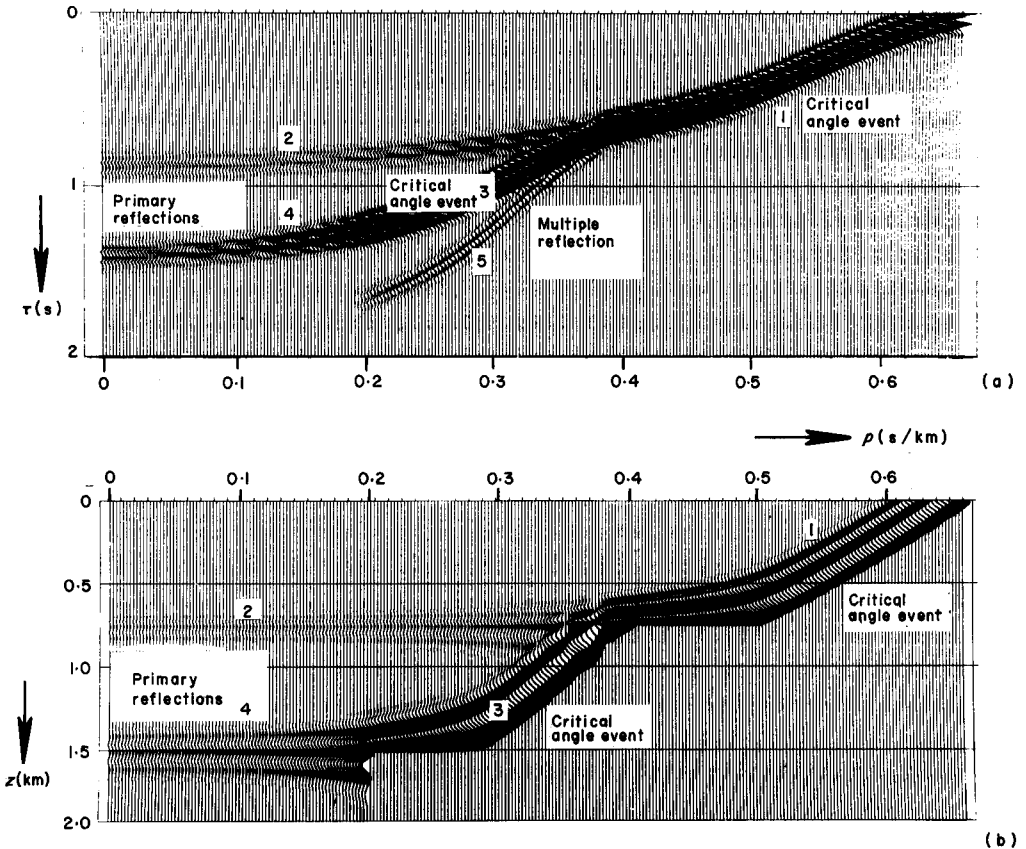


Fig. 6. Critical angle data, migrated with the WKBJ one-way wave equations. (a) Slant-stacked CSG in  $p, \tau$ -domain. (b) Migrated CSG in  $p, z$ -domain.

resents the slant-stacked CSG of fig. 4c, while fig. 6b shows the migrated data in the  $p, z$ -domain. The horizontal events (2, 4) represent the reflecting interfaces between the macro layers, while the curved events (1, 3) represent the angle dependent turning point effects [notice that the multiple reflected critical angle event (5) is not present in the migrated data because the migration procedure stops at the shallowest turning point; see step 4]. A further interpretation of fig. 6b is presented in section 7.

Finally, we remark that we derived this migration scheme from the simplified modeling scheme (5.1), where interface-related multiple reflections were neglected. In principle these multiples can be included in an iterative migration scheme based on the modeling scheme of section 2. A discussion is beyond the scope of this paper.

Berkhout (1982) gives an iterative migration scheme which properly handles multiple reflections of sub-critical angle events in 2-D and 3-D inhomogeneous media. An alternative approach to the multiple problem in migration is presented in the next section.

### 6. PRE-STACK MIGRATION SCHEME BASED ON THE TWO-WAY WAVE EQUATION

We discuss a single-record pre-stack migration scheme which includes critical angle events based on the *two-way* wave equation. We consider both ZO-imaging and PW-imaging. We follow the approach discussed in section 4. The scheme is based on inversion of the modeling scheme discussed in section 3.

In two-way wave field extrapolation techniques, upward and downward extrapolation are principally equivalent:

- (i) in upward extrapolation (modeling), downgoing waves are inversely extrapolated, while upgoing waves are forward-extrapolated simultaneously;
- (ii) in downward extrapolation (migration), downgoing waves are forward-extrapolated, while upgoing waves are inversely extrapolated simultaneously.

This means that the two-way wave field extrapolation operators discussed in part II can be applied both for modeling and migration applications. Of course, care must be taken with respect to evanescent energy. For migration in the presence of noise, spatially band-limited operators should be used. The two-way operators in the space-frequency domain discussed in part II are all band-limited operators. When applying the two-way operators in the wave number-frequency domain, then extrapolation of evanescent energy should be suppressed for stability reasons.

We assume that the macro subsurface model may be well approximated by the computational model of fig. 7. In layer  $i + 1$ , the medium properties  $c_{i+1}$ ,  $\rho_{i+1}$  can be described as the sum of constant reference properties  $\bar{c}_{i+1}$ ,  $\bar{\rho}_{i+1}$  and inhomogeneous deviation properties  $\Delta c_{i+1}$ ,  $\Delta \rho_{i+1}$ . For this computationally convenient subsurface model we propose the following recursive single record pre-stack two-way migration scheme:

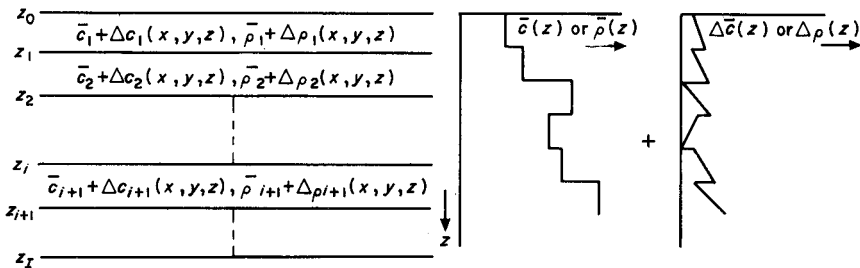


Fig. 7. A computationally convenient subsurface model for the two-way wave equation migration scheme which includes critical angle events.

1. given the total field  $\mathbf{Q}(z_i)$ , then downward extrapolation can be applied according to

$$\mathbf{Q}(z_{i+1}) = \mathbf{W}(z_{i+1}, z_i)\mathbf{Q}(z_i), \quad (6.1a)$$

with

$$\mathbf{Q} = [P, \rho^{-1} \partial_z P]^T = [P, -j\omega V_z]^T. \quad (6.1b)$$

The operator  $\mathbf{W}$  is discussed below;

2. the total wave field can be decomposed into downgoing and upgoing waves according to

$$\mathbf{P}(z_{i+1}) = \mathbf{L}^{-1}(z_{i+1})\mathbf{Q}(z_{i+1}), \quad (6.2a)$$

with

$$\mathbf{P} = [P^+, P^-]^T. \quad (6.2b)$$

The operator  $\mathbf{L}^{-1}$  is discussed below. The downgoing source wave  $S^+(z_{i+1})$  can be retrieved from the downgoing wave  $P^+(z_{i+1})$  by means of a "first arrival time window";

3. for imaging we consider two cases:

(i) ZO-imaging can be applied according to

$$\langle R(x, y, z_{i+1}) \rangle = \frac{\Delta\omega}{2\pi} \sum_{\omega} X(x, y, z_{i+1}, \omega), \quad (6.3a)$$

where

$$X(x, y, z_{i+1}, \omega) \doteq P^-(x, y, z_{i+1}, \omega)/S^+(x, y, z_{i+1}, \omega) \quad (6.3b)$$

in some stable sense. The summation is carried out for constant  $x$  and  $y$ ;

(ii) PW-imaging can be applied, according to

$$\langle \tilde{R}(p_x, p_y, z_{i+1}) \rangle = \frac{\Delta\omega}{2\pi} \sum'_{\omega} \tilde{X}(k_x, k_y, z_{i+1}, \omega), \quad (6.4a)$$

where

$$\tilde{X}(k_x, k_y, z_{i+1}, \omega) \doteq \tilde{P}^-(k_x, k_y, z_{i+1}, \omega)/\tilde{S}^+(k_x, k_y, z_{i+1}, \omega) \quad (6.4b)$$

in some stable sense. The symbol  $\sum'$  denotes that the summation is carried out for constant  $p_x = k_x/\omega$  and  $p_y = k_y/\omega$ .

Steps 1, 2 and 3, which describe the total migration procedure for one micro-layer, should be applied recursively;

4. the procedure starts at  $z = z_0$ , where the boundary condition  $\mathbf{Q}(z_0)$  follows from the CSG and the source signature. We consider two cases:

(i) At a reflection free surface  $z_0$  we may write

$$\mathbf{Q}(z_0) = \mathbf{L}(z_0)\mathbf{P}(z_0), \quad (6.5a)$$

where

$$\mathbf{P}(z_0) = [P^+(z_0), P^-(z_0)]^T. \quad (6.5b)$$

The operator  $\mathbf{L}$  is discussed below.  $P^+(z_0)$  represents the downgoing source wave  $S^+(z_0)$ , while  $P^-(z_0)$  is obtained from  $P_{\text{CSG}}^-(z_0)$  by inverting the spatial convolution

$$P_{\text{CSG}}^-(x, y, z_0, \omega) = D(x, y, z_0, \omega) * P^-(x, y, z_0, \omega) \quad (6.5c)$$

in some stable sense, where  $D(z_0)$  describes the pressure detector properties;

(ii) at a pressure free surface  $z_0$  we may write

$$\mathbf{Q}(z_0) = [P(z_0), -j\omega V_z(z_0)]^T. \quad (6.6a)$$

Here  $P(z_0)$  represents the pressure source  $S(z_0)$ , while  $V_z(z_0)$  is obtained from  $V_{z, \text{CSG}}(z_0)$  by inverting the spatial convolution

$$V_{z, \text{CSG}}(x, y, z_0, \omega) = D(x, y, z_0, \omega) * V_z(x, y, z_0, \omega) \quad (6.6b)$$

in some stable sense, where  $D(z_0)$  describes the particle velocity detector properties;

5. the procedure stops at  $z = z_I$ ;

6. in case of laterally varying reflection properties, steps 1, 2, 3(i), 4 and 5, which describe the total migration procedure for one CSG, should be repeated for all CSG's. The individual migration results can be summed afterward (true CDP-stacking), optionally after a residual NMO correction if the input velocity model is in error.

The computational diagram of this scheme is presented in fig. 8.

### Discussion

For the configuration shown in fig. 7, operator  $\mathbf{W}$  in step 1 represents the first order finite difference two-term operator  $\mathbf{W}_1^{(2)}$  in the space-frequency domain, given by (5.8) in part II. In this operator sub-critical as well as critical angle events are properly incorporated. For the special situation that lateral variations of the medium properties may be neglected, then step 1 should preferably be applied in the wave number-frequency domain, with operator  $\tilde{\mathbf{W}}$  given by (3.12) in part II. The decomposition operator  $\mathbf{L}^{-1}$  in step 2 is given by (2.6d) in part II. Unfortunately, this operator converges slowly and critical angle events are not incorporated. However, in practice it will often be sufficient to apply the decomposition in the wave number-frequency domain for the reference medium only, with operator  $\tilde{\mathbf{L}}^{-1}$  given by (3.3d) in part II. When critical angle events must be incorporated in the decomposition as well, then operator  $\tilde{\mathcal{L}}^{-1}$ , given by (3.14e) in part II should be used. It should be noted that errors in the decomposed wave field  $\mathbf{P}$  do not contribute to deeper depth levels, since the total field  $\mathbf{Q}$  is downward extrapolated independently in step 1.

In step 2 the downgoing source wave should be resolved from the total down-

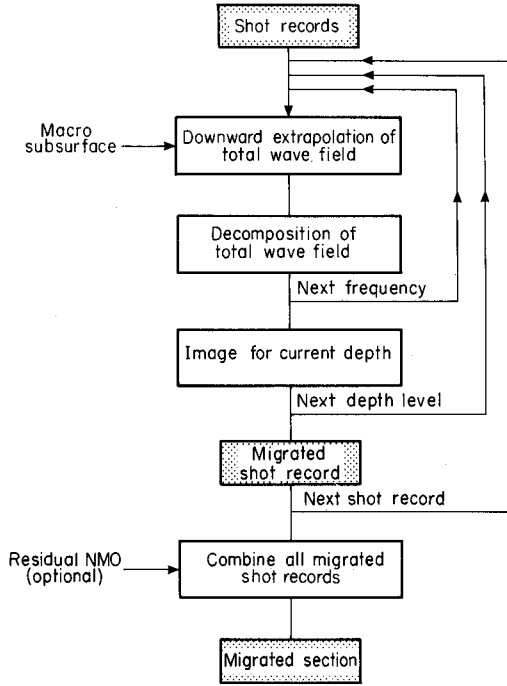


Fig. 8. Computational diagram of the shot record oriented pre-stack migration scheme, based on the two-way wave equation.

going wave in order to avoid imaging of *multiple reflections*. This will be demonstrated in an example below.

The imaging procedure in step 3 should be stabilized. This can be accomplished by approximating the ZO-impulse response according to

$$X(x, y, z_{i+1}, \omega) \cong \frac{[S^+(x, y, z_{i+1}, \omega)] * P^-(x, y, z_{i+1}, \omega)}{|S^+(x, y, z_{i+1}, \omega)|^2 + \sigma^2}, \tag{6.7a}$$

or by approximating the PW-impulse response according to

$$\tilde{X}(k_x, k_y, z_{i+1}, \omega) \cong \frac{[\tilde{S}^+(k_x, k_y, z_{i+1}, \omega)] * \tilde{P}^-(k_x, k_y, z_{i+1}, \omega)}{|\tilde{S}^+(k_x, k_y, z_{i+1}, \omega)|^2 + \sigma^2}, \tag{6.7b}$$

where  $\sigma$  represents a stabilization constant. For many practical applications amplitude errors are less important than phase errors so the scaling in (6.7a, b) may be deleted in the ZO-impulse response according to

$$X(x, y, z_{i+1}, \omega) \cong [S^+(x, y, z_{i+1}, \omega)] * P^-(x, y, z_{i+1}, \omega), \tag{6.8a}$$

or in the PW-impulse response according to

$$\tilde{X}(k_x, k_y, z_{i+1}, \omega) \cong [\tilde{S}^+(k_x, k_y, z_{i+1}, \omega)] * \tilde{P}^-(k_x, k_y, z_{i+1}, \omega). \tag{6.8b}$$

Notice that (6.8) is the frequency domain representation for the *correlation* of the downgoing source wave and the reflected upgoing waves. The composition operator  $\mathbf{L}$  in step 4(i) is given by (2.6b) in part II. For many practical applications, operation (6.5a) may be applied in the wave number-frequency domain, with  $\tilde{\mathbf{L}}$  given by (3.3b) in part II. Notice that at a pressure-free surface the composition algorithm is not required [step 4(ii)].

In case of single detector elements,  $D(x, y, z_0, \omega) = \delta(x) \delta(y) D(\omega)$ , so convolutions (6.5c) and (6.6b) may be replaced by multiplications. In this case  $P^-(z_0)$  follows from

$$P^-(x, y, z_0, \omega) = \frac{D * (\omega) P_{\text{CSG}}^-(x, y, z_0, \omega)}{|D(\omega)|^2 + \sigma^2} \quad (6.9a)$$

at a reflection-free surface [step 4(i)], while  $V_z(z_0)$  follows from

$$V_z(x, y, z_0, \omega) = \frac{D * (\omega) V_{z, \text{CSG}}(x, y, z_0, \omega)}{|D(\omega)|^2 + \sigma^2} \quad (6.9b)$$

at a pressure-free surface [step 4(ii)], where  $\sigma$  represents a stabilization constant.

The performance of the algorithm is demonstrated with some simple two-dimensional numerical examples. For simplicity we consider PW-imaging in 1-D inhomogeneous media. In this case the whole procedure can be applied in the ray-parameter frequency domain  $(p, \omega)$ .

Consider the medium shown in fig. 9a, which is bounded by a pressure-free surface at  $z_0$ . The boundary condition  $\mathbf{Q}(z_0) = [\tilde{P}(z_0), -j\omega \tilde{V}_z(z_0)]^T$  is shown in fig. 9b for one constant  $p_0$ -value (constant  $k_x/\omega$ ), such that  $\sin \theta(z_0) = p_0 c(z_0) = 0.5$ , that is, for one oblique plane wave with incidence angle  $\theta(z_0) = 30^\circ$ . Here  $\tilde{P}(z_0)$  represents the pressure source wave at  $z_0$  while  $\tilde{V}_z(z_0)$  represents the detected particle velocity at  $z_0$ . For clarity the data are shown in the ray-parameter intercept-time domain  $(p_0, \tau)$ . Notice that besides the primary reflections many multiples are present. The downward-extrapolated data  $\tilde{P}(z)$  are shown in fig. 9c for all  $z$ , again in the  $(p_0, \tau)$  domain. A similar picture could be shown for  $\tilde{V}_z(z)$ . Notice the strong resemblance with a Vertical Seismic Profile (VSP) recorded in a vertical bore hole. The decomposed data  $\tilde{S}^+(z)$  and  $\tilde{P}^-(z)$  are shown in fig. 9d and e, respectively. Notice that the downward-extrapolated upgoing waves  $\tilde{P}^-(z)$  are terminated at the reflectors; no upgoing waves are present in the lower half-space. This is a typical property of the two-way approach. Finally the imaged result is shown in fig. 9f. Notice that the image shows the two reflectors. *Multiple energy is not imaged* because the downgoing source wave  $S^+(z)$  and the upgoing multiple reflected waves in  $P^-(z)$  do not correlate.

Consider the continuously layered medium shown in fig. 10a and b, with a reflection-free surface at  $z_0$ . For one oblique plane wave with incidence angle  $\theta(z_0) = 45^\circ$ , the downward-extrapolated data  $\tilde{P}(z)$  are shown in fig. 10c. The decomposed data  $\tilde{\mathcal{P}}^+(z)$  and  $\tilde{\mathcal{P}}^-(z)$  are shown in fig. 10d and e, respectively. Finally, the imaged result is shown in fig. 10f. Notice that the image shows the turning point for the critical angle event under consideration.

Notice that in both examples the imaged results (figs 9f and 10f) represent *one*

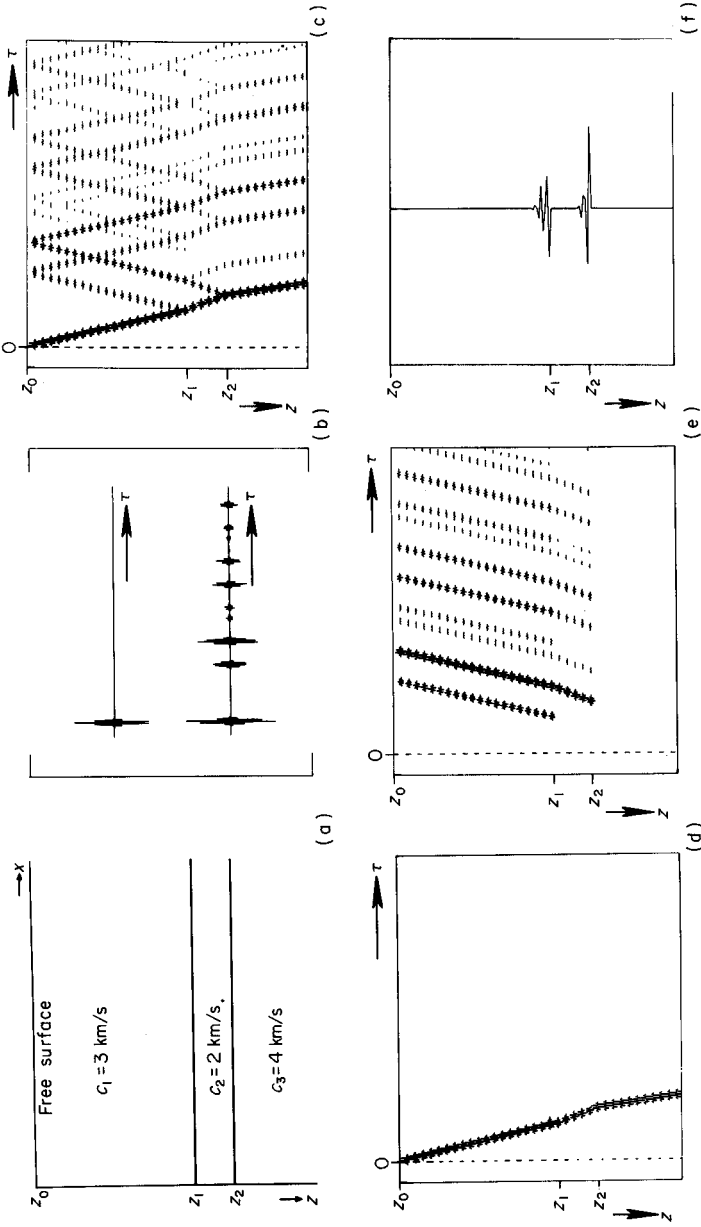


Fig. 9. Example of pre-stack two-way wave equation migration. (a) Horizontally-layered medium below a free surface. (b) Boundary condition  $\tilde{Q}(z_0)$ . (c) Downward extrapolated data  $\tilde{P}^+(z)$ . (d) Upgoing source wave  $\tilde{S}^+(z)$ . (e) Upgoing reflected waves  $\tilde{P}^-(z)$ . (f) PW-imaged result.

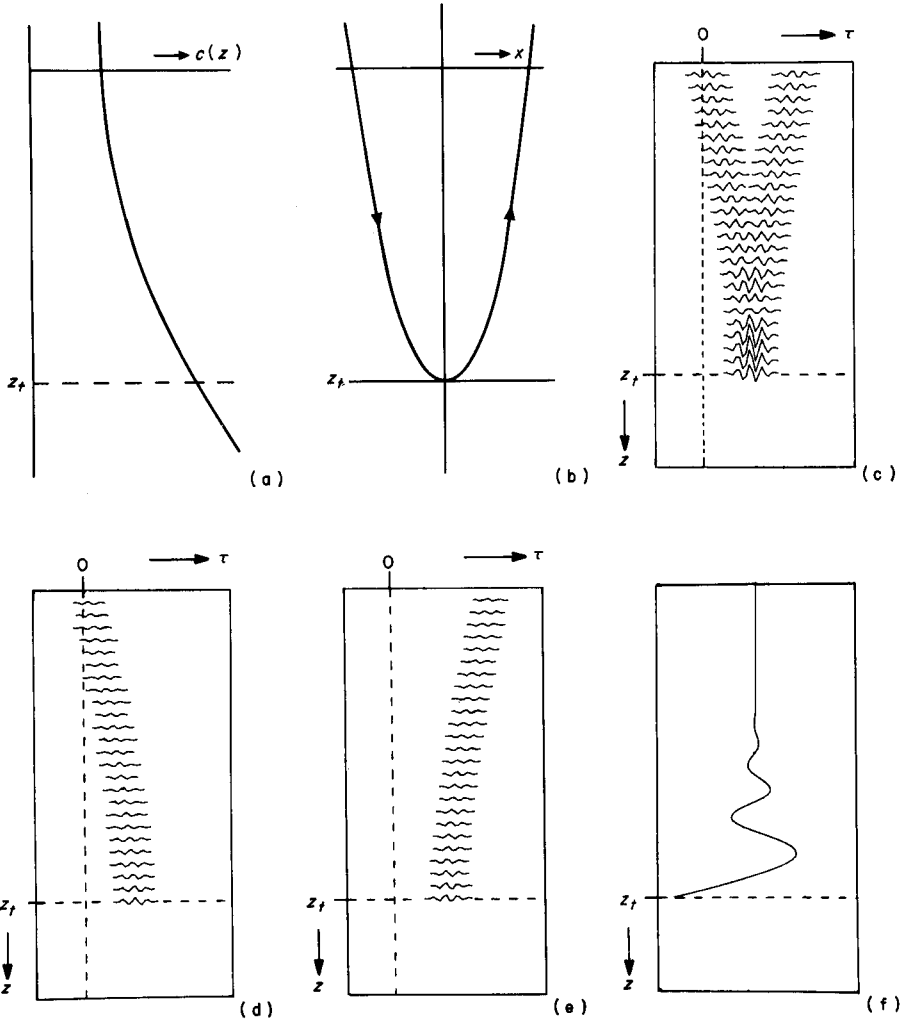


Fig. 10. Example of pre-stack two-way wave equation migration, including critical angle events. (a) Depth dependent velocity function  $c(z)$ . (b) Continuously layered medium with ray representation of a critical angle event. (c) Downward extrapolated data  $\tilde{P}(z)$ . (d) Downgoing wave  $\tilde{P}^+(z)$ . (e) Upgoing wave  $\tilde{P}^-(z)$ . (f) PW-imaged result.

angle of incidence only. If the procedure would be repeated for all angles of incidence then image representations similar to fig. 6b would be obtained.

The pre-stack migration scheme based on the two-way wave equation shows higher flexibility (2-D and 3-D inhomogeneous media) than the modeling scheme presented in section 3 (1-D inhomogeneous media). This is due to the fact that the objective of migration (impulse response at zero offset and zero time) is simpler than that of modeling (impulse response for all offsets and all times). Notice the following

advantages of the pre-stack two-way wave equation migration scheme over conventional one-way schemes:

- (i) use of the square root operator is avoided;
- (ii) a true CDP-stack is accomplished;
- (iii) transmission effects are included;
- (iv) critical angle events may be properly handled;
- (v) multiple reflected waves may be properly handled.

It is shown by Wapenaar, Kinnegeing and Berkhouit (1986b) that *converted* waves may be properly handled as well. For a proper handling of multiple reflected (and converted) waves, accurate knowledge of the subsurface model is required. As in conventional multiple elimination schemes, a small mispositioning of the major reflecting boundaries may result in an increase of undesired reflection events, so the scheme should preferably be applied iteratively. On the other hand, the generation of undesired reflection events may be avoided by spatially filtering (smoothing) the abrupt changes in the subsurface model before migration. Of course, multiple reflected (and converted) waves will then no longer be properly handled.

## 7. VELOCITY INVERSION SCHEME

A typical property of many inversion techniques is that the abrupt changes of the medium properties are retrieved from the data while inversion of the gradual changes is highly inaccurate. The reason for this is that most inversion techniques make use of sub-critical angle data only, which contain only average *propagation* information of the gradual transition zones: waves reflected by a major boundary below a gradual transition zone are transmitted through this zone. Local *reflection* information of a gradual transition zone may be obtained by involving critical angle events in the inversion process: critical angle waves are reflected at turning points inside a gradual transition zone. We discuss a simple 1-D velocity inversion scheme which includes critical angle events.

Consider again the migrated data of fig. 6b. As in section 5, the curved lines in the ray parameter-depth domain ( $p, z$ ) represent the angle dependent turning point effects. For the ray parameter we may write with Snell's law

$$p = \sin \theta(z_0)/c(z_0) = \sin \theta(z)/c(z), \quad (7.1a)$$

where  $\theta(z)$  represents the depth-dependent propagation angle. At a turning point propagation is horizontal [ $\theta(z_t) = 90^\circ$ ], so

$$p = 1/c(z_t). \quad (7.1b)$$

This means that the turning point reflection curves in the migrated data of fig. 6b may be interpreted as (reciprocal) velocity profiles in the slowness-depth domain ( $c^{-1}, z$ ) (see also fig. 11c). In other words, velocity information of a gradual transition zone may be obtained directly from migrated data which contain critical angle events. Unfortunately, this velocity information should be available beforehand in order to perform the migration properly. Using an incorrect *input* velocity

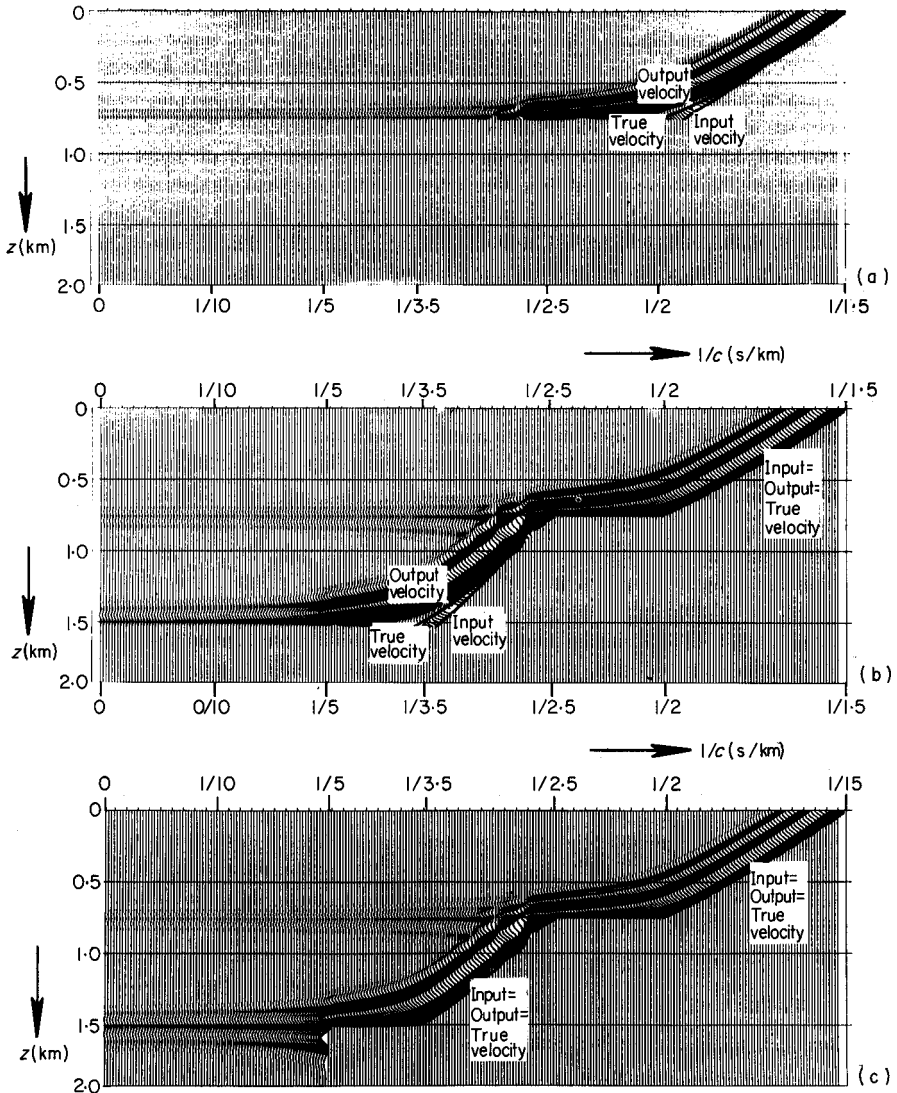


Fig. 11. Recursive velocity inversion. (a) The first macro layer is undermigrated. (b) The first macro layer is correctly migrated, the second macro layer is undermigrated. (c) Both macro-layers are correctly migrated.

profile for migration yields an incorrect (reciprocal) *output* velocity profile in the slowness-depth domain. The velocity inversion procedure described in this section aims at deriving the *true* velocity profile from the input and output velocity profiles in a non-iterative way. Clayton and McMechan (1981) proposed an inversion scheme, based on iterative migration, where the migration input velocity profile in step  $k + 1$  is equal to the average of the input and output velocity profiles in step  $k$ .

In their migration algorithm use is made of the *one-way* phase shift operator. The inversion scheme is terminated when the output velocity profile matches the input velocity profile.

Based on the migration schemes presented, we propose the following *recursive* velocity inversion scheme:

1. given the downward extrapolated data at interface  $z_m$ , migration can be applied for macro layer  $m + 1$ , according to the algorithm described in sections 5 or 6, using an estimated migration input velocity profile  $c'_{m+1}(z)$ .

2. the output velocity profile  $c''_{m+1}(z)$  can be measured from the migrated data, for instance by means of coherence calculations. From  $c'_{m+1}(z)$  and  $c''_{m+1}(z)$  the true velocity  $c(z)$  may be estimated. We consider two cases:

- (i) as in the non-recursive procedure of Clayton and McMechan (1981) we may write for our recursive inversion procedure

$$\hat{c}_{m+1}(z) = \frac{1}{2}[c'_{m+1}(z) + c''_{m+1}(z)]. \quad (7.2a)$$

Notice that this relation is biased (see appendix I). Steps 1 and 2(i) should be applied iteratively, with  $[c'_{m+1}(z)]_{\text{new}} = [\hat{c}_{m+1}(z)]_{\text{old}}$ . The iterative procedure stops when

$$|c'_{m+1}(z) - c''_{m+1}(z)| < \varepsilon, \quad (7.2b)$$

where  $\varepsilon$  represents a threshold level;

- (ii) if  $c_{m+1}^{-2}(z)$  is linear within the macro layer, the unbiased true velocity follows directly from  $c'_{m+1}(z)$  and  $c''_{m+1}(z)$ , as is shown in appendix I. Here it is assumed that  $c_{m+1}(z_m)$  is known. This value can be obtained directly from the downward-extrapolated data at interface  $z_m$ ;

3. after the velocity profile  $c_{m+1}(z)$  has been determined, the data can be downward-extrapolated to interface  $z_{m+1}$ , using either a one-way or a two-way wave field extrapolation operator including critical angle events.

Steps 1, 2 and 3, which describe the total inversion procedure for macro-layer  $m + 1$ , should be applied recursively;

4. the procedure starts at  $z = z_0$ , assuming an initial estimate  $c'(z)$  is available for all  $z$ ;

5. the procedure stops at  $z = z_M$ .

### Discussion

Compared to the scheme proposed by Clayton and McMechan (1981), notice the following refinements:

- (i) sub-critical as well as critical angle events are properly incorporated both in the migration step (step 1) and in the downward extrapolation step (step 3);  
(ii) because the scheme is applied recursively for macro layers, less iteration steps are required, particularly as the biased (7.2a) is not applied for the entire

medium, but for macro-layers only [step 2(i)]. Under a special assumption, convergence already occurs after one iteration step [step 2(ii)].

Figure 11a shows the first macro layer of the migrated CSG of fig. 4c. As the migration velocity was too low, the input and output velocity profiles do not match. Following the procedure described in appendix I, the true velocity profile for the first macro layer can be found directly. In fig. 11b, the first macro-layer was migrated, using the correct velocity profile, while the second macro-layer was undermigrated. Again the true velocity can be found directly from the input and output velocity profiles. Finally, fig. 11c shows the correctly migrated data for both macro-layers. Notice that the migrated sub-critically reflected energy is perfectly aligned, which indicates the correctness of the *average velocity* of the macro-layers. In addition, notice that the output velocity profile represented by the migrated critically reflected energy matches the input velocity profile for the entire depth range. This accounts for the correctness of the *local velocity* inside the macro-layers as well.

The 1-D velocity inversion scheme presented provides indispensable background medium information for linearized multidimensional inversion techniques, as proposed by Berkhout (1984).

## 8. CONCLUSIONS AND DISCUSSION

In principle, there are two approaches to modify the wave equation such that wave field depth extrapolation operators can be derived:

- (i) decomposition into two first-order one-way wave equations for  $P^+$  and  $P^-$ , respectively;
- (ii) reformulation into a first-order two-way matrix wave equation for  $(P, \rho^{-1} \partial P / \partial z)^T$ .

In parts I and II we discussed the theoretical aspects of both approaches. In this part we discussed the applications in modeling, migration and inversion.

### 8.A. 1-D inhomogeneous media ( $c = c(z)$ , $\rho = \rho(z)$ )

We have introduced a pre-stack modeling scheme which includes critical angle events, based on the WKB one-way wave equations (section 2). The model assumption is shown in fig. 1. We also discussed a pre-stack modeling scheme which includes critical angle events, based on the two-way wave equation (section 3). The model assumption indicated in fig. 3 is less restrictive than that indicated in fig. 1. Therefore, for critical angle modeling applications in 1-D inhomogeneous media we propose to make use of the two-way wave equation modeling scheme. The significance of the one-way wave equation modeling scheme is of theoretical nature:

- (1) it provides the basis for the pre-stack migration scheme which includes critical angle events based on the WKB one-way wave equations (section 5);
- (2) optionally, only primaries may be modeled, which is not possible with the two-way wave equation modeling scheme.

Also we introduced a pre-stack migration scheme, which includes critical angle events, based on the two-way wave equation (section 6). The latter scheme properly handles multiple reflections, but accurate knowledge of the subsurface model is required, which should be obtained iteratively. Therefore, for critical angle migration applications in 1-D inhomogeneous media we propose to make use of the WKBJ one-way wave equation migration scheme (section 5).

Finally, we discussed a velocity inversion scheme for 1-D inhomogeneous media. Based on above conclusions we propose to use the one-way wave equation migration scheme for the inversion per macro layer (steps 1 and 2). Once the velocity has

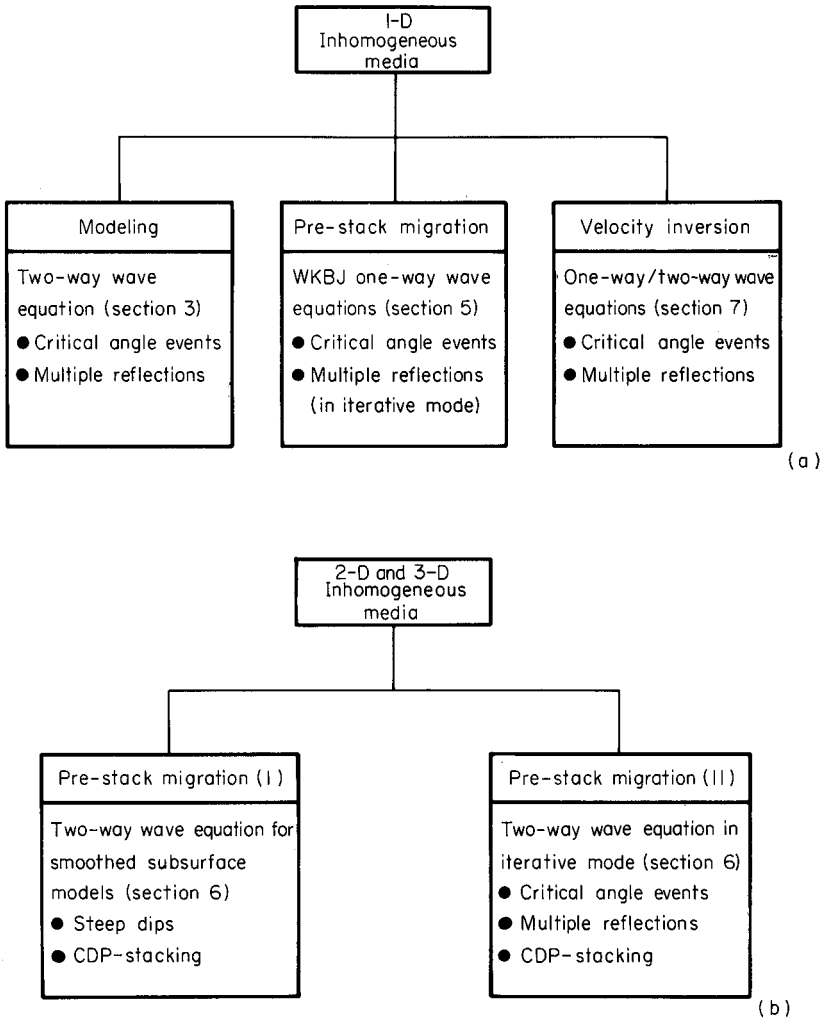


Fig. 12. Practical applications of the modeling, migration and inversion schemes, discussed in this paper. (a) Methods particularly oriented to critical angle events in piece-wise continuously layered media. (b) Pre-stack migration in arbitrary inhomogeneous media.

been properly determined for the current macro-layer, we propose to use the two-way wave field extrapolation operator for the downward extrapolation to the next macro-layer interface (step 3), such that interface related multiple reflections are properly handled.

#### 8.B. 2-D and 3-D inhomogeneous media [ $c = c(x, y, z)$ , $\rho = \rho(x, y, z)$ ]

We introduced a pre-stack migration scheme which includes critical angle events, based on the two-way wave equation (section 6). The scheme properly handles multiple reflections, but accurate knowledge of the subsurface model is required; in practical applications it should be obtained iteratively.

When inversion for multiple reflections is not required we propose to make use of the two-way wave equation migration scheme for smoothed 2-D or 3-D inhomogeneous subsurface models. A very good performance with respect to steep dips may be expected because the square root operator is avoided, while true CDP-stacking is accomplished.

Above conclusions are summarized in fig. 12. Note that we have addressed depth techniques only, i.e., those algorithms which are based on extrapolating along the depth coordinate. An interesting alternative approach to two-way wave field extrapolation is discussed by Baysal, Kosloff and Sherwood (1984). They present *post-stack* modeling and migration schemes for 2-D inhomogeneous media which make use of recursive traveltimes steps rather than depth steps. The principle of time extrapolation can easily be used for pre-stack *modeling* in 2-D (and 3-D) inhomogeneous media. A discussion is beyond the scope of this paper. The reader is referred to Kosloff and Baysal (1982). However, for pre-stack *migration* in 2-D and 3-D inhomogeneous media we prefer to make use of the depth extrapolation scheme, as discussed in this paper (section 6), because it allows simultaneous forward and inverse extrapolation of downgoing and upgoing waves (primaries as well as multiples), respectively, which is essential for a proper imaging principle.

### ACKNOWLEDGMENTS

Many thanks are due to Yann Parrod and François Beaufrière, who developed a great part of the software during a visit to Delft University sponsored by Elf Aquitaine. Also the help of Wim Kotterman with the numerical examples in section 6 is appreciated. The authors thank Hanneke Mulder for typing the three manuscripts. The investigations were supported by the Netherlands Foundation for Earth Science Research (AWON) with financial aid from the Netherlands Technology Foundation (STW).

### APPENDIX I

#### A DIRECT VELOCITY INVERSION SCHEME ASSUMING $c^{-2}(z)$ IS LINEAR IN A MACRO-LAYER

We discuss the details of step 2(ii) of the inversion scheme presented in section 7. We assume that the data are downward-extrapolated to  $z_m$ , and we abbreviate  $c_{m+1}(z)$

and  $c_{m+1}(z_m)$  to  $c(z)$  and  $c_0$ , respectively. According to Aki and Richards (1980), the intercept time  $\tau$ , corresponding to a critical angle event described by ray parameter  $p$ , can be expressed as

$$\tau(p) = 2 \int_0^{z_t(p)} \sqrt{c^{-2}(z) - p^2} dz, \quad (\text{AI.1})$$

where the turning point depth  $z_t(p)$  follows from  $p = 1/c(z_t)$ . Migrating critical angle data, using an estimated velocity profile  $c'(z)$ , yields an apparent turning point depth  $z'_t(p)$  which satisfies the following integral equation:

$$2 \int_0^{z_t(p)} \sqrt{c^{-2}(z) - p^2} dz = 2 \int_0^{z'_t(p)} \sqrt{[c'(z)]^{-2} - p^2} dz. \quad (\text{AI.2})$$

The underlying philosophy for this equation is that the turning point image is obtained when the intercept time  $\tau$  is consumed by means of downward extrapolation of the data. In the following we present a solution of (AI.2), assuming

$$c^{-2}(z) = c_0^{-2}[1 - az], \quad a > 0. \quad (\text{AI.3a})$$

Furthermore, we assume that the data are migrated, using migration velocity  $c'(z)$ , such that

$$[c'(z)]^{-2} = c_0^{-2}(1 - a'z), \quad 0 < a' \leq a. \quad (\text{AI.3b})$$

Finally, we assume that the output velocity profile  $c''(z)$  satisfies

$$[c''(z)]^{-2} = c_0^{-2}[1 - a''z], \quad a'' \geq a. \quad (\text{AI.3c})$$

Notice that, with  $p = 1/c(z_t)$ , the corresponding turning point depths follow from

$$z_t(p) = [1 - c_0^2 p^2]/a, \quad (\text{AI.4a})$$

$$z'_t(p) = [1 - c_0^2 p^2]/a', \quad (\text{AI.4b})$$

$$z''_t(p) = [1 - c_0^2 p^2]/a''. \quad (\text{AI.4c})$$

Given the input and output parameters  $a'$  and  $a''$ , respectively, the true value  $a$  follows from (AI.2)–(AI.4), according to

$$a = a' / \left[ 1 - \left( 1 - \frac{a'}{a''} \right)^{3/2} \right]. \quad (\text{AI.5})$$

Now the true velocity is obtained by substituting this value in (AI.3a).

Notice that even for  $|1 - a'/a''| \ll 1$  we may *not* write  $a \approx \frac{1}{2}(a' + a'')$ , so (7.2a) is biased, even for small gradients, which follows from rewriting (AI.3) for small gradients.

## REFERENCES

- AKI, K. and RICHARDS, P.G. 1980, *Quantitative Seismology*, W.H. Freeman and Company, San Francisco.

- BAYSAL, E., KOSLOFF, D.D. and SHERWOOD, J.W.C. 1984, A two-way nonreflecting wave equation, *Geophysics* 49, 132–141.
- BERKHOUT, A.J. 1982, *Seismic Migration*, Vol. 14A, Elsevier, Amsterdam.
- BERKHOUT, A.J. 1984, Multi-dimensional linearized inversion and seismic migration, *Geophysics* 49, 1881–1895.
- CLAYTON, R.W. and McMECHAN, G.A. 1981, Inversion of refraction data by wave field continuation, *Geophysics* 46, 860–868.
- DE GRAAFF, M.P. 1984, Pre-stack migration by single shot record inversion, Doctoral Thesis, Delft University of Technology, Delft.
- KENNETT, B.L.N. and ILLINGWORTH, M.R. 1981, Seismic waves in a stratified half space—III. Piecewise smooth models, *Geophysical Journal of the Royal Astronomical Society* 66, 633–675.
- KOSLOFF, D.D. and BAYSAL, E. 1982, Forward modeling by a Fourier method, *Geophysics* 47, 1402–1412.
- LOEWENTHAL, D., LU, L., ROBERSON, R. and SHERWOOD, J. 1974, The wave equation applied to migration, *Geophysical Prospecting* 24, 380–418.
- WAPENAAR, C.P.A. and BERKHOUT, A.J. 1985, Wave field extrapolation techniques for inhomogeneous media which include critical angle events, Part I, Methods using the one-way wave equations, *Geophysical Prospecting* 33, 1138–1159.
- WAPENAAR, C.P.A. and BERKHOUT, A.J. 1986a, Wave field extrapolation techniques for inhomogeneous media which include critical angle events, Part II, Methods using the two-way wave equation, *Geophysical Prospecting* 34, 147–179.
- WAPENAAR, C.P.A., KINNEGING, N.A. and BERKHOUT, A.J. 1986b, Principle of pre-stack migration based on the full elastic two-way wave equation, submitted for publication in *Geophysics*.

## ERRATA

### WAVE FIELD EXTRAPOLATION TECHNIQUES FOR INHOMOGENEOUS MEDIA WHICH INCLUDE CRITICAL ANGLE EVENTS, PARTS I-III

by C.P.A. WAPENAAR and A.J. BERKHOUT

Part I: Methods Using the One-Way Wave Equations, vol. 33, no. 8, December 1985, pp. 1138–1159.

Page 1153, relation (7.4b):  $\tilde{P}^-$  should read as  $\tilde{\mathcal{P}}^-$ .

Part II: Methods Using the Two-Way Equation, vol. 34, no. 2, April 1986, pp. 147–179.

Page 156: relations (3.6a) and (3.6b) should read as

$$\tilde{W}(z, z_0) = \mathbf{I} + \tilde{\mathbf{L}}(\tilde{\mathbf{A}} \Delta z)\tilde{\mathbf{L}}^{-1} + \frac{1}{2} \tilde{\mathbf{L}}(\tilde{\mathbf{A}} \Delta z)\tilde{\mathbf{L}}^{-1}\tilde{\mathbf{L}}(\tilde{\mathbf{A}} \Delta z)\tilde{\mathbf{L}}^{-1} + \dots, \quad (3.6a)$$

$$\tilde{W}(z, z_0) = \tilde{\mathbf{L}}[\mathbf{I} + (\tilde{\mathbf{A}} \Delta z) + \frac{1}{2} (\tilde{\mathbf{A}} \Delta z)^2 + \dots]\tilde{\mathbf{L}}^{-1}. \quad (3.6b)$$

Part III: Applications in Modeling, Migration and Inversion, vol. 34, no. 2, April 1986, pp. 180–207.

Page 184, last line: (3.9) should read as (3.12).

Page 190–197: the symbol \* should read as a superscript (denoting complex conjugation) in the following relations: (5.4), (5.6), (6.7), (6.8) and (6.9).